Cell Motility and the Cytoskeleton 59:264–272 (2004)

The Tail of Myosin Reduces Actin Filament Velocity in the In Vitro Motility Assay

Bin Guo and William H. Guilford*

Department of Biomedical Engineering, University of Virginia, Charlottesville

It has been observed that heavy meromyosin (HMM) propels actin filaments to higher velocities than native myosin in the in vitro motility assay, yet the reason for this difference has remained unexplained. Since the major difference between these two proteins is the presence of the tail in native myosin, we tested the hypothesis that unknown interactions between actin and the tail (LMM) slow motility in native myosin. Chymotryptic HMM and LMM were mixed in a range of molar ratios (0–5 LMM/HMM) and compared to native rat skeletal myosin in the in vitro motility assay at 30°C. Increasing proportions of LMM to HMM slowed actin filament velocities, becoming equivalent to native myosin at a ratio of 3 LMM/HMM. NH_4^+-ATPase assays demonstrated that HMM concentrations on the surface were constant and independent of LMM concentration, arguing against a simple displacement mechanism. Relationships between velocity and the number of available heads suggested that the duty cycle of HMM was not altered by the presence of LMM. HMM prepared with a lower chymotrypsin concentration and with very short digestion times moved actin at the same high velocity. The difference between velocities of actin filament propelled by HMM and HMM/LMM decreased with increasing ionic strength, suggesting that ionic bonds between myosin tail and actin filaments may play a role in slowing filament velocity. These data suggest the high velocities of actin filaments over HMM result from the absence of drag generated by the myosin tail, and not from proteolytic nicking of the motor domain. Cell Motil. Cytoskeleton 59:264–272, 2004.

Key words: heavy meromyosin; light meromyosin; motility assay; ATPase assay; ionic strength

INTRODUCTION

The in vitro motility assay is a powerful tool for studying the function and properties of myosins [Kron and Spudich, 1986; Toyoshima et al., 1987; Uyeda et al., 1990, 1991; Kron et al., 1991; Harris and Warshaw, 1993]. Previous studies used either native myosin [Kron and Spudich, 1986; Warshaw et al., 1990; Harris and Warshaw, 1993] or its enzymatic derivatives, heavy meromyosin (HMM) and S1 [Toyoshima et al., 1987; Uyeda et al., 1991; Kron et al., 1991], all of which support actin filament motion, though at markedly different velocities. It has been shown that the velocity of actin filaments on an HMM-coated nitrocellulose surface is higher than that on native myosin, while the actin filaments move slower on S1 than on myosin [Toyoshima et al., 1987; Kron et al., 1991]. The basis for these differences remains unclear. Toyoshima et al. [1987] suggested that the different velocities could be explained by the different physical orientation of these species on the nitrocellulose surface. Myosin and HMM may bind to the surface via the long tail and S2 portion, respectively, such that most

Contract grant sponsor: National Institutes of Health; Contract grant numbers: AR45604 and HL64381.

*Correspondence to: William H. Guilford, Department of Biomedical Engineering, University of Virginia, Charlottesville, VA 22908.
E-mail: guilford@virginia.edu

Received 24 May 2004; accepted 14 September 2004

Published online in Wiley InterScience (www.interscience.wiley.com).
DOI: 10.1002/cm.20040

of the heads are free above the surface to interact with actin filaments and generate power strokes. However, by definition S1 molecules must bind to the surface directly by the head. Thus, while S1 heads bound to the surface may bind to actin filaments, they might not generate complete power strokes [Toyoshima et al., 1987]. The higher velocities of actin filaments over HMM compared to native myosin are more difficult to explain. Kron et al. [1991] suggested that the increased average velocity for HMM was associated with proteolytic nicking at sites within the myosin head when modifications of the protocol were made to increase HMM yield from myosin.

However, since the major difference between native myosin and HMM is the tail (rod, or light meromyosin, LMM) of native myosins, it is possible that unknown interactions exist between actin filaments and the tail that may slow motility. Although it has been reported that myosin rods do not bind to actin at relatively high ionic strength [Cooke and Franks, 1978], when bound to the hydrophobic nitrocellulose surface the tail may denature and enable non-native interactions between the tail and actin filaments. Further, motility assays are ordinarily performed at low ionic strength, which may allow non-physiologic interactions between actin and LMM. These interactions may exert a drag force on the filaments and slow motility in native myosin below that of HMM.

To test this hypothesis, LMM was mixed with HMM at various molar ratios and tested in the in vitro motility assay. We found that LMM slowed actin filament velocities over HMM without affecting the density of HMM heads on the motility surface or the duty cycle of the individual motors. Velocities became equivalent to native myosin at a molar ratio of 3 LMM/HMM. The difference between velocities produced by HMM and HMM/LMM mixture decreased with increasing ionic strength and vanished at about physiological ionic strength (~180 mM). These data suggest that ionic interactions between LMM and actin are the cause of reduced actin filament velocities of native myosin relative to HMM.

MATERIALS AND METHODS

Protein Preparation

G-Actin (99% purity) from rabbit skeletal muscle (Cytoskeleton, Denver, CO) was polymerized and labeled with TRITC-phalloidin (Sigma, St.Louis, MO) according to manufacturer's instructions.

Myosin was prepared from rat hindleg muscle according to Shiverick et al. [1975] with minor modifications. Briefly, 100 mg muscle tissue was minced thoroughly by a tissue tearor (Model 985370, Biospec Products, Inc.) in 1 ml extraction buffer (300 mM KCl, 10 mM HEPES, 10 mM $Na_4P_2O_7 \cdot 10\ H_2O$, 1 mM $MgCl_2$, 10 mM DTT, 1 mM ATP, pH 6.8), and was stirred on ice for 60–90 min. Supernatant was collected after spinning the extract 1 h at 140,000*g*. Two volumes of 1 mM DTT (pre-chilled on ice) were added to the supernatant and the mixture was left on ice for 1 h. Myosin was removed by spinning the mixture at 20,000*g* for 20 min and the precipitate was dissolved into 200 μl of storage solution (0.6 M KCl, 50 mM potassium phosphate buffer, pH 6.8). This myosin (≈10 mg/ml) was used immediately to prepare heavy meromyosin (HMM) and light meromyosin (LMM), or stored at −20°C in 50% (v/v) glycerol.

HMM and LMM were prepared essentially as described [Margossian and Lowey, 1982]. Briefly, chymotrypsin (10 mg/ml in 0.001 N HCl, Sigma, St. Louis, MO) was added to myosin (10 mg/ml) to a final concentration of 0.05 mg/ml and incubated at room temperature for 6 min. The reaction was stopped by adding 0.1 M PMSF (Sigma) in 70% ethanol to a final concentration of 0.5 mM. The digestion mixture was then dialyzed against low salt buffer (25 mM KCl, 25 mM Imidazole, 1 mM EGTA, 4 mM $MgCl_2$, 1 mM DTT) overnight at 4°C followed by centrifugation at 200,000*g* for 30 min. The HMM supernatant was collected. The pellet, which contained LMM and undigested myosin, was resuspended in 200 μl of high salt buffer (0.6 M KCl, 50 mM potassium phosphate, pH 7.0) and 3 volumes of 95% ethanol (4°C) were added to it. The mixture was stirred on ice for 2–3 h to irreversibly denature the undigested myosin. The precipitate was collected by centrifugation at 20,000*g* for 30 min, resuspended in 500 μl of high salt buffer (described above) and dialyzed against this same buffer with frequent changes overnight at 4°C. After centrifugation at 200,000*g* for 30 min, the supernatant was collected and dialyzed again against low salt buffer (25 mM KCl, 25 mM Imidazole, 1 mM EGTA, 4 mM $MgCl_2$, 10 mM DTT, pH 7.4) overnight at 4°C. The precipitated LMM was then collected by centrifugation at 20,000*g* for 30 min and resuspended in small volume of myosin buffer (300 mM KCl, 25 mM Imidazole, 1 mM EGTA, 4 mM $MgCl_2$, pH 7.4).

In a separate experiment, same amount of myosin was digested for varying periods of time (0.5, 2, 6, 15, 30, 60 min) at a final chymotrypsin concentration of 0.02 mg/ml. HMM from each digestion was then purified as described above. HMM from 6 min digestion of myosin at 0.05 mg/ml chymotrypsin (as above) served as a control.

Protein concentrations were determined with Advanced Protein Assay Reagent (Cytoskeleton, Denver, CO) according to the manufacturer's instructions. Purity was assessed by electrophoresis on NuPAGE™ 4–12%

Bis-Tris gel in MOPS running buffer and the gel was then stained by Simply Blue™ SafeStain according to the manufacturer's instructions (Invitrogen, Carlsbad, CA). Both HMM and LMM were stored in liquid nitrogen as 50% (v/v) glycerol to allow thawing on ice.

In Vitro Motility Assay

Motility was measured with myosin, HMM and HMM/LMM mixtures using standard in vitro motility assay methods [Warshaw et al., 1990; Uyeda et al., 1991; Kron et al., 1991] at 30°C. Briefly, myosin or HMM or HMM/LMM mixture in high salt buffer (300 mM KCl, 25 mM Imidazole, 1 mM EGTA, 4 mM $MgCl_2$, 10 mM DTT, pH 7.4) was applied to a flow cell constructed from a nitrocellulose-coated coverslip and glass slide. Myosin and HMM were applied with a final concentration of 50 and 30 μg/ml, respectively, such that they were equimolar. If HMM/LMM was used, HMM and LMM were mixed in a range of molar ratios (0–5 LMM/HMM) so that the final concentration of HMM was always 30 μg/ml. After a 1-min incubation, the flow cell was blocked with 1% BSA (Sigma) in low salt buffer (25 mM KCl, 25 mM Imidazole, 1 mM EGTA, 4 mM $MgCl_2$, 10 mM DTT, pH 7.4) for 1 min, followed by TRITC-phalloidin labeled actin filaments, and two washes. Actin filament movement was assayed in low salt motility buffer (25 mM KCl, 25 mM Imidazole, 1 mM EGTA, 4 mM $MgCl_2$, 10 mM DTT, 1 mM ATP, 0.5% Methylcellulose, pH 7.4) except where specified. The motility buffer also contained an oxygen scavenger system (0.125 mg/ml Glucose oxidase, 0.0225 mg/ml Catalase, 2.87 mg/ml Glucose).

Tracking Algorithm

The median velocities of moving filaments (scalar velocities, equivalent to speed) and moving fraction of filaments (fraction of total that move) were determined using a centroid-based algorithm incorporated into a plug-in for ImageJ (developed at the United States National Institutes of Health by Wayne Rasband and available on the Internet at http://rsb.info.nih.gov/ij/). Movies of in vitro motility were created at 10 frames per second for 30 frames. In ImageJ one selects the filaments using the threshold tool, and invokes the plug-in. Two results matrices are created, one for each of two subsequent image slices (e.g., frame 1 and frame 2), and the built-in particle analysis routines are called to fill the matrices with the centroid, area and perimeter of each selected object (filament). The algorithm then seeks the filament in frame 2 with a position closest to that of a given filament in frame 1. It is assumed that even when moving, an object will still be closer to its original position than to any other object in the field of view. However, since close encounters between objects still occur, two additional constraints are applied. The identified filament in frame 2 must also have the same perimeter and shape index (SI) as the original, within a certain tolerance. The shape index is defined as

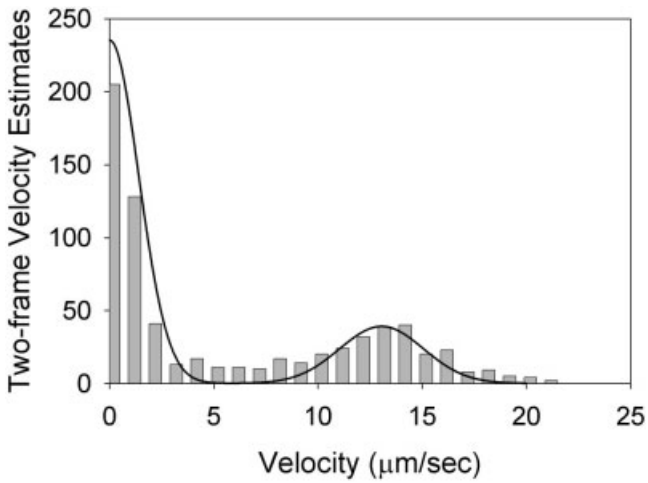

Fig. 1. Histogram of individual two-frame velocity estimates from a single movie. Also shown is the fit of a pair of Gaussians to the data. One Gaussian is constrained to center on a velocity of zero to represent the non-moving population of filaments. The center of the second Gaussian provides the modal velocity of the moving population.

$$\mathrm{SI} = 4\pi A/P^2 \quad (1)$$

where A is the particle area and P is the particle perimeter [McDonald, 1994]. SI varies between 1 for a round object and 0 for a line. If the tolerances are met for perimeter and shape index (15% typical), a velocity is calculated from the separation of the centroids and the time interval between frames, and an entry is made into a velocity histogram (1 μm/sec bins for these data). Otherwise, the particle is ignored, and the next particle in frame 1 is used to find a match in frame 2. This process continues for all the objects in frame 1, and subsequently for comparisons of frame 2 to frame 3, and so on. When this process is completed, one is left with a histogram of individual two-frame velocity estimates (Fig. 1). The histogram typically contains a peak at $\leq$1 μm/sec representing non-moving objects, and a second peak representing the most common velocity of moving filaments. The sum of a pair of Gaussians is fit to the data by the simplex method, with one being forced to center on 0, representing the non-moving population. The center point of the second Gaussian is the most common (modal) velocity of filaments in that movie. One may also estimate the moving fraction of filaments (f_M) by the magnitudes (areas) of the moving and non-moving Gaussian peaks, M and M_O respectively.

$$f_M = M/(M + M_0/2) \quad (2)$$

M_0 is divided by two in this equation because while the Gaussian is centered on zero, only the positive half of the curve actually exists. Finally, one may derive a useful estimate of the equivalent number (N) of filaments that would be tracked from the first frame to the last as an account of the number of individual velocity measurements. This value of N is calculated simply as the number of individual velocity estimates divided by the number of frames, minus one. Modal velocities from replicate experiments are averaged to give a mean velocity and calculate the standard error of the mean.

In practice, this algorithm is extraordinarily fast (7 frames per second on a 1-GHz PC) and reproduces the results calculated by hand using cross-correlation tracking [Cheezum et al., 2001] to within experimental error. It is also insensitive to "losing track" of a filament for one or more frames, and to filaments that enter or leave the field of view. This is because our matching algorithm, described above, does not attempt to segment the image and track filaments over extended frames. There are, however, certain limitations. The algorithm can report unrealistically high velocities if the frame rate is too low compared to the filament velocity, or if the density of filaments in the field of view is too high. This is because the probability is increased that the algorithm will incorrectly accept a neighboring filament as its match in the subsequent frame. Second, the calculated fraction moving is typically an underestimate by 10% or more. This is due to (1) fluorescent artifacts that are included as nonmoving filaments, (2) the fact that a good match is easier to make when a filament doesn't move, and (3) failure of the fit curves to account for all the moving filaments. Finally, this algorithm only describes the aggregate behavior of a large number of filaments, and does not report the behavior of individual filaments. It should also be noted that while centroid estimates are adequate for rough measures of motion spanning many pixels, subpixel estimates are fraught with error [Cheezum et al., 2001].

Persistence Length Measurements

The persistence length was measured for surface-associated actin filaments in the in vitro motility assay in the presence and absence of LMM (no HMM or myosin). The contour length of a filament was measured and its instantaneous end-to-end length was also measured frame by frame using ImageJ. From the contour length and the instantaneous end-to-end length, its instantaneous persistence length was calculated [Howard, 2001; equation 6.13]. The mean variances of the persistence lengths of the two conditions were compared. We also measured the frame-to-frame displacement along one axis (x) of one end of each filament in order to calculate a diffusion coefficient as $D = \langle x^2 \rangle / 2\Delta t$.

ATPase Assay

HMM head density was estimated using an NH_4^+-EDTA ATPase assay [Chalovich and Eisenberg, 1982; Harris and Warshaw, 1993]. In solution, HMM was incubated at a final concentration of 2 μg/ml in 150 μl NH_4^+-EDTA ATPase buffer (0.4M NH_4Cl, 2 mM EDTA, 25 ml Tris, 0.2M sucrose, 1 mM DTT, 1 mM ATP, and 1 mg/ml BSA, pH 7.4) at 30°C. The reaction was terminated by adding 150 μl stop solution (58 mM EDTA, pH 6.5, 6.6% SDS) at various times. ATPase rates were then estimated colorimetrically after adding 600 μl color development solution (0.5% Ammonium molybdate, 0.5% $FeSO_4 \cdot 7H_2O$, 0.5M H_2SO_4) to the stopped reaction mixture [White, 1982]. Absorbance was read at 700 nm.

The ATPase rates of HMM bound to the flow cell were similarly measured. HMM or HMM/LMM mixture was applied to the flow cells and blocked with BSA as described in the in vitro motility assay, except that there was no $MgCl_2$ in these buffers; NH_4^+-EDTA ATPase buffer was introduced into the flow cells that were then incubated at 30°C for various periods of time. Stop solution was flowed through and the effluent was collected and assayed as described above. The ATPase rates of bound HMM were compared to those of HMM in solution. The HMM head density on the coverslip was estimated assuming that the NH_4^+-EDTA ATPase rate of HMM heads bound to coverslips is the same as that in solution.

Duty Cycle Estimation

Rat skeletal muscle HMM duty cycle (f) was estimated by the approach as described [Harada et al., 1990; Uyeda et al., 1990; Harris and Warshaw, 1993]. A moving actin filament experiences both the propelling force by HMM and the drag force due to surrounding solution. Since the drag force is much smaller than the propelling force and the latter of a single HMM head is sufficient to move an actin filament at maximum velocity (V_{max}), an actin filament can move at V_{max} when at least one HMM head is bound and undergoing power stroke at any instance. Assuming the interaction between actin and HMM heads is stochastic, the probability that an actin filament is propelled by at least one stroking head is given by

$$P = 1 - (1 - f)^N \quad (3)$$

where N is the total number of HMM heads that are able to interact with the actin filament [Harada et al., 1990; Uyeda et al., 1990; Harris and Warshaw, 1993]. At low HMM densities, P is relatively low; therefore, the experimental velocity (V) of an actin filament is given by the product of V_{max} and the probability shown above:

$$V = (\alpha \times V_{max}) \times [1 - (1 - f)^N] \quad (4)$$

where α is the efficiency of force transmission [Uyeda et al., 1990; Harris and Warshaw, 1993]. In this model, the duty cycle is defined as the fraction of time that a myosin head is undergoing power stroke.

To estimate the duty cycles for both HMM and HMM/LMM mixtures, the in vitro motility assay was performed with HMM alone at a concentration of 20 μg/ml and with HMM/LMM mixture (molar ratio of LMM/HMM = 2:1, [HMM] = 20 μg/ml). In each case, an individual actin filament's length and velocity were measured. Velocities were measured using a cross-correlation algorithm [Cheezum et al., 2001] in an ImageJ plugin. The length and HMM head density were used to calculate *N*. According to the band model by Uyeda et al. [1990] and Harris and Warshaw [1993], we assumed that as an actin filament passed over an HMM-coated surface, all HMM heads within a 26-nm-wide band centered at the center of the filament could interact with the filament. Therefore, *N* is given by the product of the HMM head density measured previously by the ATPase assay, 26 nm, and the filament length. Knowing the velocity (*V*) and *N* for each filament, *V* was plotted as a function of *N*, and equation 4 was fitted to the data (Sigmaplot, SPSS) with $\alpha \times V_{max}$ and the duty cycle *f* being the two free parameters [Uyeda et al., 1990; Harris and Warshaw, 1993].

RESULTS

Protein Preparation

Purified HMM and LMM were stained by Simply Blue™ SafeStain (Invitrogen, Carlsbad, CA) after SDS-PAGE. Proteins were overloaded to visualize contamination. There was slight LMM contamination in HMM, but there was no detectable HMM contamination in LMM (Fig. 2).

HMM Density on the Coverslip

NH_4^+-EDTA ATPase rate for rat skeletal HMM was measured by the amount of inorganic phosphate (Pi) released. In solution, this rate was found to be 1,123 Pi/head/min at 30°C, which agreed with previously reported values (1,140 Pi/head/min at 30°C) [Uyeda et al., 1990]. HMM at various concentrations (5–80 μg/ml) were applied to flow cells and their ATPase rates were measured. These ATPase rates were then converted to HMM head densities on the coverslip assuming the same rate of Pi release per head as in solution. For HMM concentrations up to 40 μg/ml, head density on nitrocellulose coated coverslip was a linear function of the HMM concentration applied (Fig. 3).

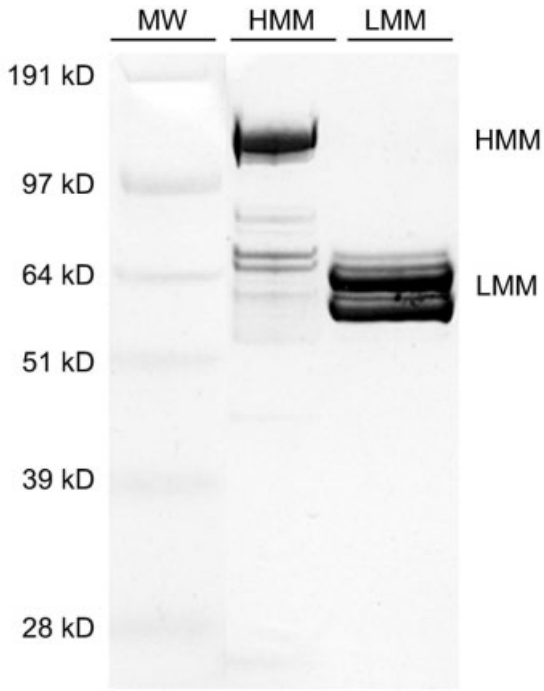

Fig. 2. SDS-PAGE of HMM and LMM preparation; 5 μg HMM and >10 μg LMM were loaded. No contamination of HMM can be observed in the LMM preparation.

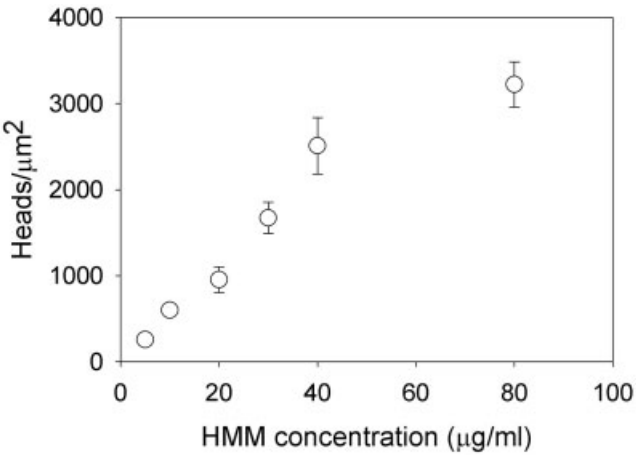

Fig. 3. HMM head density on nitrocellulose-coated coverslips as a function of HMM concentration applied. There is a linear relationship between head density and concentration up to 40 μg/ml. Error bars represent standard error of the mean in all figures.

To determine if the presence of LMM affects the density of HMM on the motility surface, measurements of NH_4^+-EDTA ATPase rate were conducted under the same conditions for an LMM/HMM mixture, in which HMM was at 40 μg/ml and LMM was at 30 μg/ml (approximately 2:1 LMM/HMM molar ratio). NH_4^+-EDTA ATPase rate for this mixture was not changed compared to that for HMM (40 μg/ml) alone. Conse-

quently, the HMM density for this LMM/HMM mixture was 2,584 ± 286 (mean ± sem) heads/μm^2, close to 2,509 ± 328 heads/μm^2 for HMM (40 μg/ml) alone. This head density agreed well with 2,400 heads/μm^2 measured by Uyeda et al. [1990].

HMM Duty Cycle

The duty cycle (*f*) of HMM was estimated by the method of Uyeda et al. [1990]. The in vitro motility assay was performed with HMM alone and HMM/LMM mixture. The LMM concentration was 15 μg/ml and in both cases HMM concentration was 20 μg/ml (2:1 LMM/HMM). Velocity and filament length were measured for each individual actin filament, and the maximum number (*N*) of HMM heads available to interact with each actin filament was estimated from the head density as described in Materials and Methods. The actin filament velocities (*V*) versus the number of heads (*N*) for both cases were well fitted by equation 4 (Fig. 4). From these fits, duty cycles were estimated to be 0.71 ± 0.03 % for HMM alone and 0.84 ± 0.07 % for the HMM/LMM mixture.

Effects of Digestion Time

HMM prepared using different digestion times in 0.02 mg/ml chymotrypsin were tested in the in vitro motility assay. HMM from 6 min digestion of myosin by 0.05 mg/ml chymotrypsin served as control and moved actin at 11.14 ± 0.2 μm/sec. We found that HMM from digestion times up to 30 min moved actin at almost the same velocity as did control HMM (Fig. 5). However, HMM from a very prolonged digestion time (1 h) moved actin at an elevated velocity of 12.87 ± 0.16 μm/sec. This higher motility might be a consequence of proteolytic nicking of the motor domain, but as we show here, it occurs only with very prolonged digestions.

Effects of LMM on Velocity

HMM and LMM were mixed in a range of molar ratios (0–5 LMM/HMM) with constant HMM concentration and average actin filament velocities were measured for each mixture. Increasing proportions of LMM to HMM slowed actin filament velocities. At a ratio around 3 LMM/HMM, the velocity became close to that for native myosin at the same molar concentration as HMM (Fig. 6). Interestingly, the fraction of moving filaments for each LMM/HMM mixture remained constant and similar to that for pure HMM. Neither was there any change in filament length with the presence of LMM. A similar mixture experiment performed with native myosin also showed a decrease in velocity by 19% when mixed in a 1:1 molar ratio with LMM.

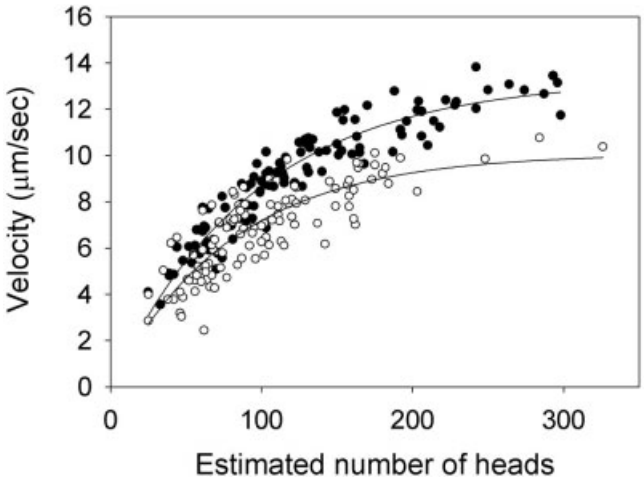

Fig. 4. HMM duty cycle was not altered by the presence of LMM. Actin filaments velocities were plotted as a function of the number of HMM heads. *Solid circles* represent actin filament velocities over HMM-coated surface ([HMM] = 20 μg/ml). *Open circles* represent actin filament velocities over HMM/LMM mixture coated surface ([HMM] = 20 μg/ml, [LMM] = 15 μg/ml, LMM:HMM ≈ 2:1 molar ratio). Equation 2 was fitted to the data (*solid lines*). From these fits, duty cycles were found to be 0.71 ± 0.03 % for HMM alone and 0.84 ± 0.07 % for HMM/LMM mixture.

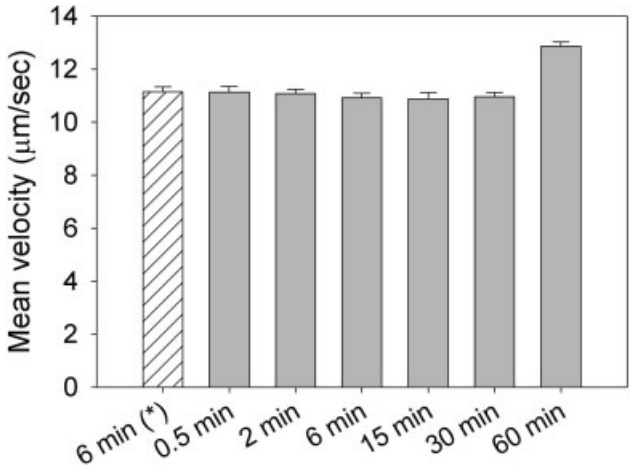

Fig. 5. Actin velocities over HMM from different digestion times; 10 mg/ml myosin was digested by 0.02 mg/ml chymotrypsin for various periods of time, except the *hatched bar* on the plot where 0.05 mg/ml for 6 min is indicated. Only at a digestion time of 1 h was there a difference in velocity for the HMM compared with the 0.05-mg/ml, 6-min control.

It is also worthy of mention that when no protein is adsorbed to a motility assay surface, some actin filaments loosely associate with the surface and undergo Brownian motion. However, if LMM alone was adsorbed to the surface, the number of actin filaments associated with the surface increased only slightly but the Brownian motion of these filaments was greatly reduced with a diffusion coefficient of 0.0062 ± 0.0026 μm^2/sec compared to that

of 1.02 ± 0.28 μm^2/sec when no LMM or HMM was applied to the surface. The variance of the instantaneous persistence length of surface-associated actin filaments also dropped significantly in the presence of LMM, 12.2 μm^2 compared to 86.8 μm^2 without any LMM or HMM. These results suggest that the LMM preparation alone does not bind actin filaments tightly to the motility surface, but it does interact with actin filaments in some way.

To further eliminate the possibility of rigor heads contamination, LMM was co-sedimented with F-actin in high salt buffer without ATP, and the experiments were repeated. Any remaining rigor myosin heads should sediment with the F-actin, leaving the supernatant with LMM alone. Cosedimentation did not change the in vitro actin filament velocities at any molar ratio of LMM/HMM. Therefore, it is unlikely that rigor head contamination is a cause of the reduced actin filament velocity with the presence of LMM. Further, electrophoresis of the F-actin pellet showed no significant cosedimentation of LMM, suggesting there are no interactions between these two molecules at high ionic strength (data not shown).

Effect of Ionic Strength on Velocity

Effect of ionic strength on actin filament velocity was tested by varying KCl concentration in the motility buffer (5–145 mM KCl). Motility was measured for actin filaments on both HMM ([HMM] = 30 μg/ml) and HMM/LMM mixture ([HMM] = 30 μg/ml, [LMM] = 20 μg/ml) at each ionic strength. As shown in Figure 7, mean velocities increase with increasing ionic strength for both cases up to an ionic strength of 78 mM. As the ionic strength increases beyond 78 mM, mean velocities decrease. Further, at high ionic strengths the difference in velocities produced by HMM and HMM/LMM mixture decreases and finally vanishes at physiological ionic strength (~180 mM).

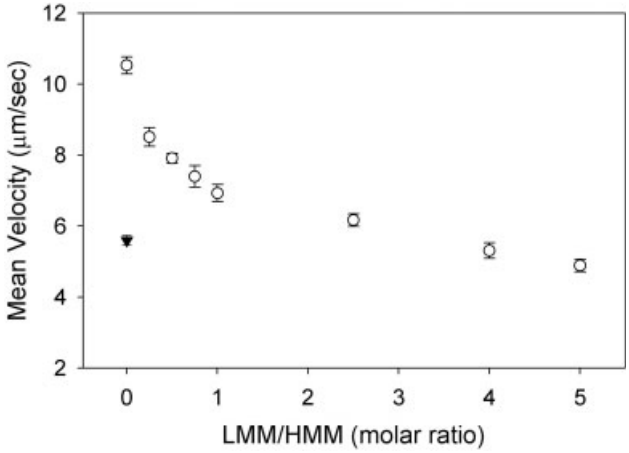

Fig. 6. Effect of LMM on actin filament velocities. HMM and LMM were mixed in a range of molar ratios (0–5 LMM/HMM) and compared to native myosin in the in vitro motility assay. Increasing proportions of LMM to HMM slowed actin filament velocities, becoming equivalent to native myosin (*arrowhead*) at a ratio of about 3 LMM/HMM. *Open circles* represent HMM/LMM mixtures at different molar ratios.

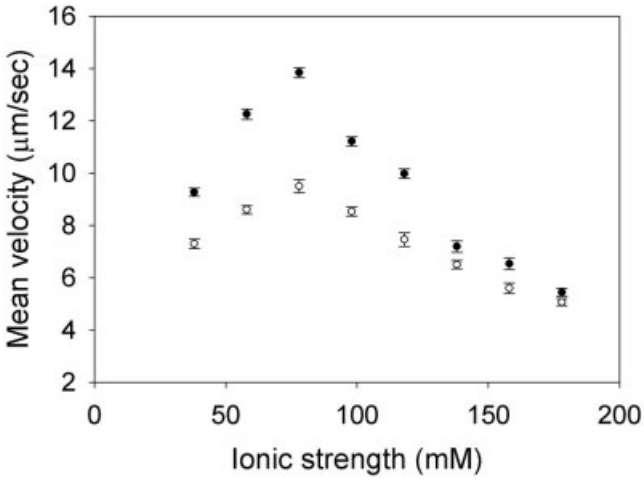

Fig. 7. Effect of ionic strength on actin filament velocity produced by HMM (*solid circles*) and HMM/LMM mixture (*open circles*). HMM concentration was 30 μg/ml in both HMM and the mixture; LMM concentration was 20 μg/ml in the mixture. Only uniformly moving filaments, regardless of their velocity, size, or brightness, were selected and measured for both cases.

DISCUSSION

We have shown that LMM can slow actin filament velocities in the in vitro motility assay. Since HMM moves actin filaments at a much higher velocity than does native myosin, and since the major difference between these two proteins is the tail of the native myosin, it is natural to suspect that velocities are in some way related to the presence or absence of the tail. The surprising conclusion of this study is that LMM need not be part of the intact myosin molecule to exert this effect.

We mixed HMM and LMM in a series of molar ratios to find at which ratio can this mixture mimic native myosin. A 1:1 ratio of HMM/LMM would represent native myosin, but this is not true once the mixture is applied to the motility surface. In the case of native myosin, heads and tails co-localize. This is in contrast to a 1:1 HMM/LMM mixture at the same sub-saturating concentration. Tails need not co-localize with heads, and their binding efficiencies may differ. Therefore, when HMM instead of myosin binds to an actin filament, there is less chance that the actin filament will interact with a tail, and one would expect a higher actin filament velocity. We found that a ~1:3 HMM/LMM mixture could

move actin filaments at the same velocity as did native myosin, suggesting that at this ratio HMM and LMM were distributed on the surface such that a moving actin filament could interact with LMM with equal probability as for native myosin.

Under unloaded conditions, the actin filament sliding velocity is determined primarily by the step displacement and attached time of myosin, which is in turn related to the rate of ATP hydrolysis and the duty cycle. It is possible that in the motility assay, the tail of myosin interacts with its own or neighboring myosin heads and thus alters their mechanochemical properties. However, our experimental results showed that the duty cycle of HMM did not change with the presence of LMM on the surface, arguing the mechanochemical properties of the myosin were not altered.

It has been suggested in the literature [Kron et al., 1991] and discussed privately amongst practitioners of the motility assay that the high actin velocity over HMM is due to proteolytic nicking of the head. However, when we digested myosin at a lower chymotrypsin concentration for a very short time (~30 sec), the resulting HMM still moved actin at the same high velocity. Only at a digestion time of 1 h did the resulting HMM move actin at an even higher speed. This is consistent with the observations of Kron et al. [1991] that excessive digestion of HMM causes a velocity increase. However, our data suggest it is unlikely that normal chymotryptic digestion conditions result in high HMM speeds because of proteolytic nicking of the motor domain.

These findings leave few possibilities other than specific or nonspecific interactions between actin filaments and the tail. Indeed, the presence of LMM alone greatly reduced the Brownian motion of actin filaments on a blank motility surface. Further, at a constant HMM concentration, addition of LMM to the motility surface slowed actin filaments, suggesting the actin filaments experienced a drag force due to LMM molecules. Together, these findings strongly indicate the existence of interactions between actin and LMM at low ionic strength. Because velocity differences disappeared at high ionic strength, it is likely these interactions are electrostatic and non-physiologic.

An alternative explanation for our data is that LMM is contaminated by rigor HMM heads, and that it is the rigor head that slows motility. However, the SDS-PAGE gel (Fig. 2) of HMM and LMM preparation shows no detectable myosin or HMM contamination of our LMM. Further, removal of rigor heads from LMM by co-sedimentation with F-actin did not change our results. Therefore, rigor head contamination is not a likely explanation for the reduced velocity caused by LMM, especially given the low molar ratios used here.

CONCLUSIONS

For obvious reasons, it is often assumed that the velocities of native myosins in the in vitro motility assay are more physiologically relevant than those of HMM. That is, it has been assumed that actin velocities on HMM are artificially faster because HMM is a proteolytic fragment of native myosin and perhaps modified in some functionally unpredictable manner. However, our data suggest that interactions between actin and myosin tail exist under the non-physiological conditions of the motility assay and disappear at physiological ionic strengths. This suggests that actin velocities over intact myosin in the standard motility assay are not a better representation of the in vivo state. Instead, in the assays using HMM, actin filaments truly interact with the heads only, making HMM a better representation under standard motility assay conditions.

ACKNOWLEDGMENTS

The authors acknowledge the constant support of the Department of Biomedical Engineering and the Cardiovascular Research Center at the University of Virginia.

REFERENCES

Chalovich JM, Eisenber E. 1982. Inhibition of actomyosin ATPase activity by troponin-tropomyosin without blocking the binding of myosin to actin. J Biol Chem 257:2432–2437.

Cheezum MK, Walker WF, Guilford WH. 2001. Quantitative comparison of algorithms for tracking single fluorescent particles. Biophys J 81:2378–2388.

Cooke R, Franks KE. 1978. Generation of force by single-headed myosin. J Mol Biol 120:361–373.

Harada Y, Sakurada K, Aoki T, Thomas DD, Yanagida T. 1990. Mechanochemical coupling in actomyosin energy transduction studied by in vitro movement assay. J Mol Biol 216: 49–68.

Harris DE, Warshaw DM. 1993. Smooth and skeletal muscle myosin both exhibit low duty cycles at zero load in vitro. J Biol Chem 268:14764–14768.

Howard J. 2001. Mechanics of motor proteins and the cytoskeleton. Sunderland, MA: Sinauer Associates, Inc. p 110–115.

Kron SJ, Spudich JA. 1986. Fluorescent actin filaments move on myosin fixed to a glass surface. Proc Natl Acad Sci USA. 83:6272–6276.

Kron SJ, Toyoshima YY, Uyeda TQP, Spudich JA. 1991. Assays for actin sliding movement over myosin-coated surfaces. Methods Enzymol 196:399–416.

Margossian SS, Lowey S. 1982. Preparation of myosin and its subfragments from rabbit skeletal muscle. Methods Enzymol 85: 55–71.

McDonald DM. 1994. Endothelial gaps and permeability of venules in rat tracheas exposed to inflammatory stimuli. Am J Physiol 266:L61–L83.

Shiverick KT, Thomas LL, Alpert NR. 1975. Purification of cardiac myosin. Application to hypertrophied myocardium. Biochim Biophys Acta 393:124–133.

Toyoshima YY, Kron SJ, Mcnally EM, Niebling KR, Toyoshima C, Spudich JA. 1987. Myosin subfragment-1 is sufficient to move actin filaments in vitro. Nature 328:536–539.

Uyeda TQP, Kron SJ, Spudich JA. 1990. Myosin step size: Estimation from slow sliding movement of actin over low densities of heavy meromyosin. J Mol Biol 214:699–710.

Uyeda TQP, Warrick HM, Kron SJ, Spudich JA. 1991. Quantized velocities at low myosin densities in an in vitro motility assay. Nature 352:307–311.

Warshaw DM, Desrosiers JM, Work SS, Trybus KM. 1990. Smooth muscle myosin cross-bridge interactions modulate actin filament sliding velocity in vitro. J Cell Biol 111:453–463.

White HD. 1982. Special instrumentation and techniques for kinetic studies of contractile systems. Methods Enzymol 85:698–708.